Induced Europium Circularly Polarised Luminescence Monitors Reversible Drug Binding to Native α_1-Acid Glycoprotein

Laura Jennings, Ryan S. Waters, Robert Pal and David Parker*

Department of Chemistry, Durham University, South Road, Durham DH1 3LE, UK

david.parker@dur.ac.uk

Abstract

The competitive binding to α_1-acid glycoprotein of a dynamically racemic europium(III) complex with seven pharmacologically active drugs absorbing in the range 250 to 290 nm, has been monitored by following changes in europium total emission and in induced circularly polarised luminescence (CPL). Binding affinities corresponding to K_d values in the range 0.5 to 100μM were measured, in good agreement with literature data.

Keywords europium; luminescence; CPL; drug binding; chirality

Introduction

Alpha-1-acid glycoprotein (α_1-AGP) is an important glycoprotein found in the plasma. It has a molecular weight of 41-43 kDa and comprises a single chain of 183 amino acids, with five N-linked oligosaccharides (glycans). [1] The carbohydrate content makes up 45% of the protein's total molecular weight. It is an acute-phase protein and the blood plasma concentration of the protein increases in response to inflammation. α_1-AGP has a normal plasma concentration between 0.6-1.2 mg/mL, representing 1-3% of the total blood plasma protein concentration. Following an acute phase reaction (e.g. stress, inflammation, burn or infection), the α_1-AGP concentration in blood can increase up to 400% from its normal concentration.

It exists as a mixture of two or three genetic variants. [1] Two genetic polymorphs are the A and the major (70%) F_1S variants; in the A variant, 22 amino acids out of 183 residues differ from the F_1S polymorph. The differences in structure of the polymorphs translate into slightly different drug binding properties. For example, α_1-AGP has an isoelectric point (p*I*) of 2.7-3.0, and predominantly binds to neutral and basic drugs[2-5] such as methadone, [2] chlorpromazine and disopyramide. [3,4]

A wide range of drugs is known to bind to α_1-AGP. Increased binding of pharmacologically active drugs to α_1-AGP moderates their clinical effect, due to decreased levels of unbound drug in the bloodstream. Such behaviour has important

clinical ramifications, for example in anaesthesia duration and in determining dosage for drug therapy. Representative examples of such drugs that bind to α_1-AGP (Fig. 1), include the heroin substitute, methadone, [6] the important tyrosine kinase inhibitor Imatinib [7] (or Gleevec) used successfully to treat chronic myelogeneous leukaemia, disopyramide- an anti-arrythmic agent used to treat ventricular tachycardia,[8] common anaesthetics, such as lidocaine and bupivacaine, [9,10] and various tricyclic anti-depressants, such as nortriptyline and imipramine. [9,11]

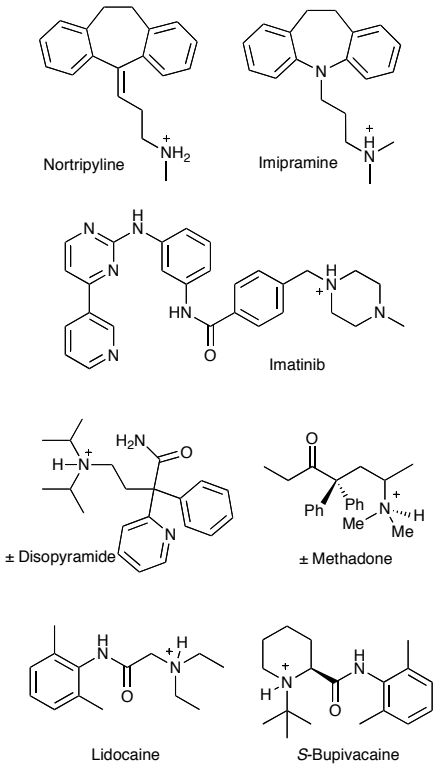

Figure 1. Selected drugs known to bind to α_1-AGP

The racemic europium complex $[Eu.L^{\mathbf{1}}(OH_2)]^{+}$, (Scheme 1), has been shown to bind reversibly to α_1-AGP {log*K* = 5.73 (0.06)}.[1,13] Addition of α_1-AGP to $[Eu.L^{\mathbf{1}}(OH_2)]^{+}$ caused displacement of the bound water molecule and gave rise to major changes in the intensity and form of the europium emission spectrum, consistent with a significant change in the coordination environment, notably involving loss of the axial donor ligand. It was hypothesised that coordination of the side-chain carboxylate of the protein Glu-64 residue had occurred, [1] consistent with structural alignment studies highlighting the presence of 3 proximate glutamate residues (Glu-35, 36 and 64 – the nearest one) in the main drug binding site of α_1-AGP.

The electronic circular dichroism (ECD) spectra of $[Eu.L^{1}(OH_2)]^{+}$ in the absence and presence of one equivalent of α_1-AGP showed two major bands at 290 and 340 nm with negative Cotton effects, typical of a well-defined coordination environment. Each transition possessed fine structure with two bands evident, which suggests that the two azaxanthone ligands are in different but rigid local environments. Such observations led to the prediction that one azaxanthone ligand had dissociated from the metal centre and was included in the hydrophobic protein binding cavity, whilst the other remained coordinated to europium, (Scheme 1). The incremental addition of chlorpromazine to the protein-bound adduct, [Eu.L**1**.AGP], caused a decrease in the induced ECD of the azaxanthone chromophore, consistent with reversible binding of $[Eu.L^{1}(OH_2)]^{+}$ to α_1-AGP, and competitive binding of chlorpromazine with the complex.

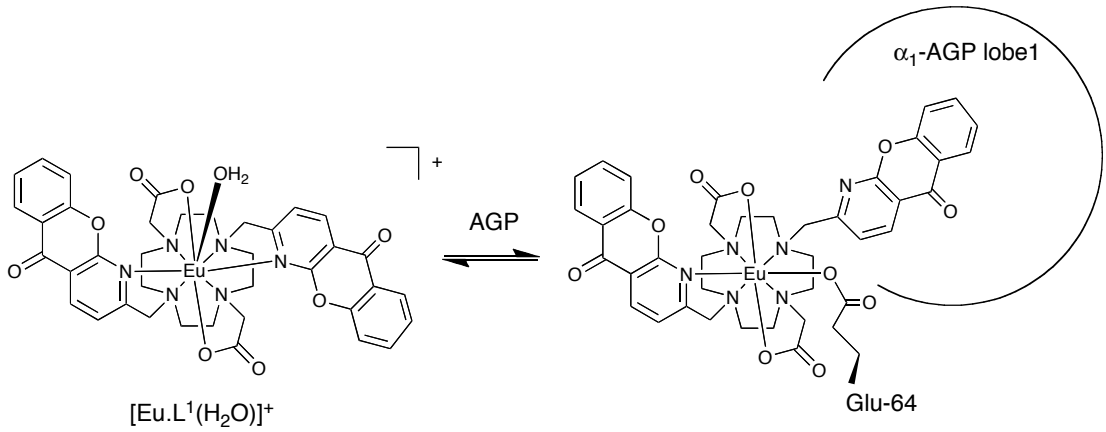

Scheme 1. Reversible binding of the complex to α_1-AGP

Binding to α_1-AGP was characterized by a switching on of a large induced europium circularly polarized luminescence (CPL). [12] The parent complex is dynamically racemic and shows no CPL. The protein bound form creates a chiral environment in which a large CPL signal is induced, following selective formation of the chiral adduct. The binding behaviour allowed the concentration of α_1-AGP to be assessed directly in serum samples. The emission changes were calibrated to read protein concentration directly and compared very favourably to independent ELISA assays. [12]

The CPL technique has many advantages when studying chiral systems, notably its high sensitivity in comparison to other chiroptical techniques, such as electronic circular dichroism. The development of lanthanide complexes as CPL probes has

gained momentum recently, as much brighter chiral complexes have been discovered. Large g_{em} values characterize the chiroptical behavior of these complexes, with g_{em} being described by equation 1. [13]

$$g_{em}(\lambda) = \frac{2\Delta I(\lambda)}{I_l(\lambda)+I_R(\lambda)} \qquad (1)$$

The long-lifetime of the luminescence allows the lanthanide complex to be observed selectively using time-gating. The emissive state of the lanthanide is also highly sensitive to the coordination environment of the complex, so changes due to reversible binding of different ligands can be observed, made simpler by the separation of the left and right-handed polarised light intensity. Thus far, many of the reported examples of lanthanide CPL probes have been qualitative rather than quantitative descriptors, showing a response of either an induced CPL signal or the loss of one. They have, however, been used in a variety of ways. Some examples take advantage of the chirality in the ligand to induce a CPL signal. Examples include the use of naturally chiral molecules such as sugars to achieve this. [13c] Others, such as that shown in Scheme 1, bind to proteins which enforces the complex to adopt a preferred low-energy conformation, and hence a strong CPL signal is induced. [12]

With this background in mind, the range of drugs shown above (Figure 1) presents an ideal set of compounds to examine the competitive binding to α_1-AGP of the drug and the europium complex. Each drug does not absorb above 320 nm allowing the Eu complex to be addressed by selective excitation into the azaxanthone chromophore, permitting sensitized emission. The binding affinity of the Eu complex for AGP (log K = 5.7) falls in the range of reported AGP binding constants for each of these systems (log K values range from 4.3 to 6.4). [6-11] Accordingly, we report that CPL can be used to assess quantitatively drug binding to a protein. The values obtained by CPL have been compared to those assessed by ratiometric analysis of total emission spectral changes. The use of CPL to monitor binding *quantitatively* either to the metal centre or via interaction of the ligand is relatively rare. [13]

Results and Discussion

The competitive binding of selected drugs (Figure 1) to the pre-formed complex, [Eu.L**1**.AGP], was monitored by studying the spectral changes in the total and CPL

emission. Each titration was set up and carried out in the same manner. The free complex (30 μM) was dissolved in aqueous NaCl solution (1 mL, 0.1 M) and α_1-AGP was added to the solution to give a 1:1 (complex:AGP) ratio. The pH was adjusted to 7.4 and initial emission and CPL spectrum were acquired. Incremental additions of the drug were made, maintaining the pH at 7.4 (I = 0.1 NaCl; 295K). Each titration was halted after ten equivalents of the drug had been added ([drug] = 300 μM) and the final emission and CPL spectra were recorded. The total emission intensity reduced in magnitude and the significant changes in spectral form permitted ratiometric analysis to be undertaken, measuring the change in the ΔJ =2/ΔJ =1 intensity ratio as a function of the concentration of added drug, (Table 1). Parallel experiments were attempted with the terbium analogue, [14] but the protein-bound complex was significantly more quenched by charge transfer, and the less strong observed emission signal -in both CPL and total emission- precluded detailed quantitative studies.

Table 1. Selected physicochemical data and estimated apparent binding constants (0.1 M NaCl, pH 7.4) for pharmaceuticals binding to native α_1-AGP.

Pharmaceutical	pK_a	λ_{max}/nm	log K [c] (tot. emission)	log K [b] (CPL)	log K [a] (literature)
(±)Methadone	8.94	270	5.34(05)	5.35(04)	5.6
(±)Bupivacaine	8.21	263	4.77(05)	5.38(03)	5.7
S-Bupivacaine	8.21	263	5.41(04)	5.46(04)	5.4
Imatinib	8.27	292	5.82(06)	5.77(04)	6.4
(±)Disopyramide	10.4	254	5.55(05)	4.99(02)	5.6
Imipramine	9.50	250	4.18(02)	4.90(04)	4.9
Nortriptyline	10.1	240	3.60(01)	4.44(04)	4.5
Lidocaine	8.19	263	4.31(03)	4.38(04)	4.4

[a] values were taken from literature references, referring to the native protein where possible [6-11]; [b] CPL data were analysed by plotting (ΔI_{max}–ΔI) as a function of added drug concentration; [c] errors quoted here refer to statistical data fitting analysis only; data analysis related to changes in the ratio of the europium ΔJ =2/ΔJ =1 emission intensity as a function of added drug (see ESI).

Overall, the most significant changes occurred in the hypersensitive ΔJ = 2 and ΔJ = 4 manifolds. In parallel, the reduction in the CPL emission intensity at 621 nm was

plotted as a function of drug concentration. (Figures 1-3; Table 1 and SI). The CPL intensity variation was also assessed at 613 nm and gave near identical data, within the estimated error. Binding isotherms derived from CPL and total emission data were analysed assuming a 1:1 binding stoichiometry for the interaction of the drug at the major AGP binding site; such a stoichiometry is consistent with literature precedent. [6-11]

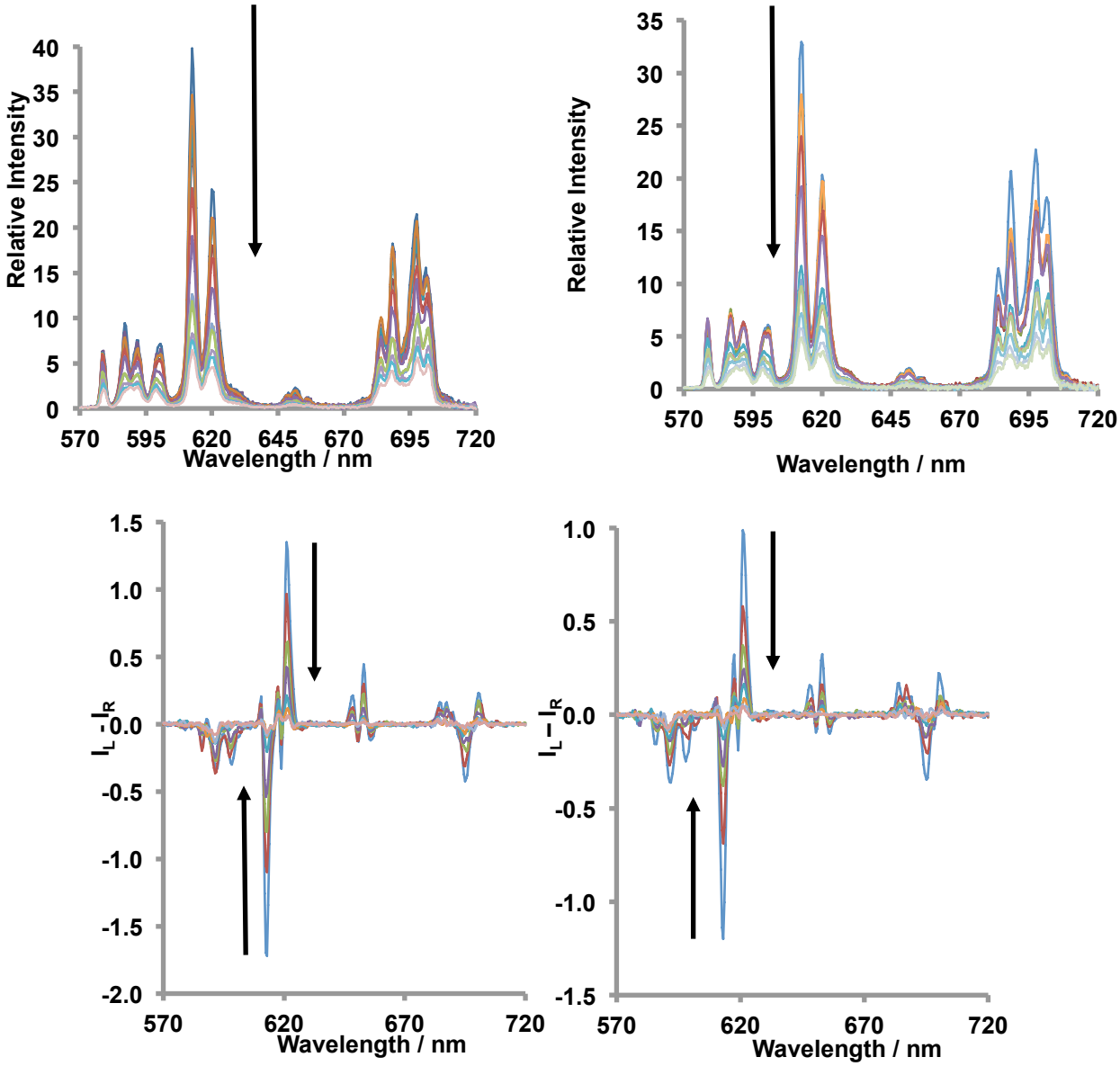

Figure 1. Variation in the total emission (*upper*) and CPL profile (*lower*) of 1:1 (Eu complex:AGP) upon addition of 0 to 300 μM racemic bupivacaine (*left*) and *S*-bupivacaine (*right*) (30 μM complex, 30 μM AGP, 295 K, pH 7.4, 0.1 M NaCl).

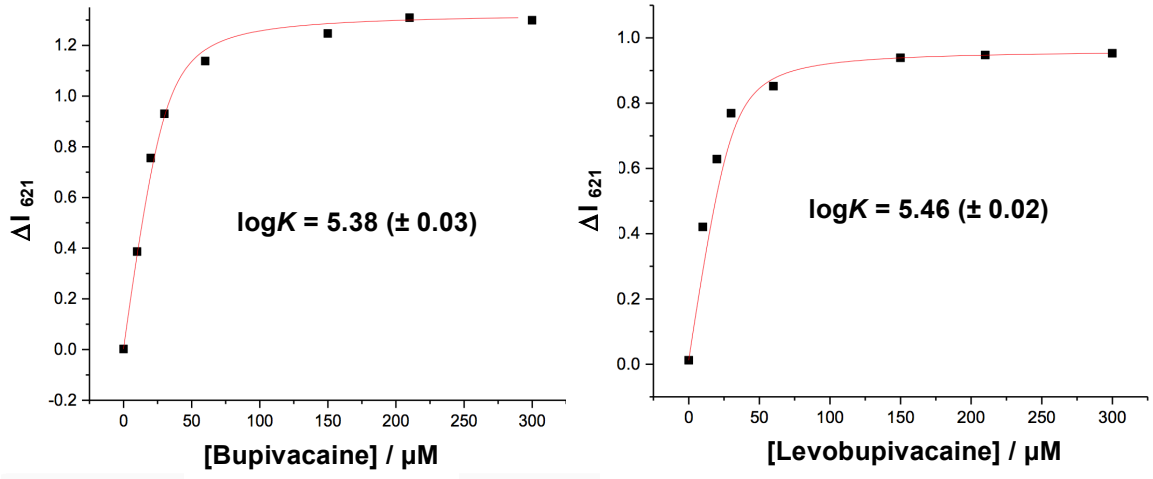

Figure 2. Competitive binding plots of $[(I_L\text{-}I_R)_{max} - (I_L\text{-}I_R)]$ (621 nm) *vs.* concentration for bupivacaine (left) and *S*-bupivacaine (right) (30 μM complex, 30 μM AGP, 295 K, pH 7.4, 0.1 M NaCl). (Bupivacaine limiting values: $LV_{min} = 0$, $LV_{max} = 1.3$) (*S*-bupivacaine limiting values: $LV_{min} = 0$, $LV_{max} = 1.0$)

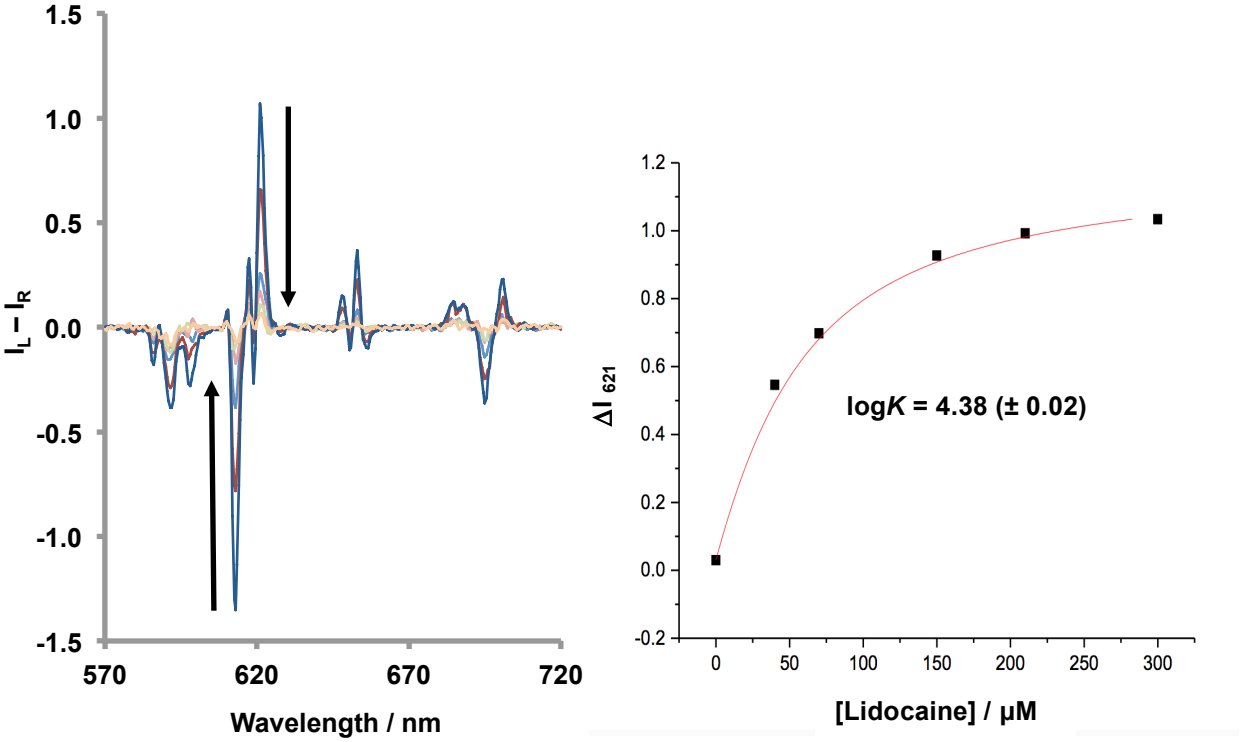

Figure 3. *Left*: variation in the CPL profile of 1:1 (Eucomplex:AGP) upon addition of 0 to 300 μM lidocaine. *Right*: competitive binding plot of $[(I_L\text{-}I_R)_{max} - (I_L\text{-}I_R)]$ (at 621 nm) *vs.* concentration of lidocaine (30 μM complex, 30 μM AGP, 295 K, pH 7.4, 0.1 M NaCl). (Lidocaine limiting values: $LV_{min} = 0$, $LV_{max} = 1.1$)

The binding of the drug to α_1-AGP first involves the dissociation of the complex from the protein binding site, followed by association of the drug into the binding pocket. The europium CPL and total emission changes provide information on the first

dissociative step only. The CPL data set relates to the change in concentration of the most emissive chiral species, whereas the total emission changes report on the weighted sum of all emissive Eu species, in proportion to their brightness and mole fraction. Nevertheless, the determination of these apparent binding constant values gives insight into the relative affinity of the drug molecule to α_1-AGP, allowing a comparison with literature data. Such published data were often obtained by monitoring the small changes in the protein CD that accompany drug binding.

Each titration was repeated twice and an average value is given. The main source of error in the CPL experimental data can be traced to the CPL detector response, in which the signal is only reliable when it is five times larger than the background noise. However, the quoted error on the binding constants derives from the fitting function, and so is an underestimate of the true error.

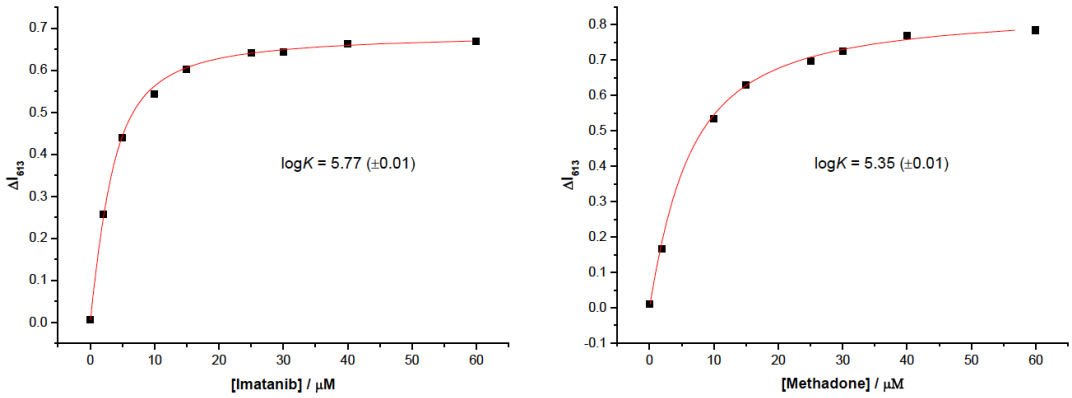

Figure 4. Competitive binding plot of $[(I_L\text{-}I_R)_{max} - (I_L\text{-}I_R)]$ (at 613 nm) *vs*. concentration of Imatinib (*left*) and methadone (*right*), (30 μM complex, 30 μM AGP, 295 K, pH 7.4, 0.1 M NaCl).

Summary

Drug binding to a protein has been studied quantitatively for the first time, using changes in circularly polarized luminescence. For the series of anaesthetics, lidocaine bound most weakly, and there was evidence from the total emission behaviour that *S*-bupivacaine bound more strongly than the racemate. Levobupivacaine is the (*S*)-enantiomer of bupivacaine and a similar apparent binding constant to native AGP was calculated in each case, although the literature binding constant to AGP is reported to be slightly higher for racemic bupivacaine than for the S enantiomer (log K = 5.72 vs

5.43). [10b,10c] However, another study has suggested that *S*-bupivacaine has a higher affinity towards the F_1S variant of AGP than racemic bupivacaine, with log*K* values of 5.84 (± 0.02) and 5.52 (± 0.03) respectively. The F_1S variant normally constitutes 70% of the total AGP, and so usually is the more important to consider.[14] Therefore, some caution needs to exercised in interpreting these data. [10a] Of the remaining systems analysed, imipramine bound more strongly than the related nortriptyline, whilst the more hydrophobic imatinib, bound most strongly, in accord with literature binding data.

Conclusions

The competitive binding to α_1-acid glycoprotein of the selected pharmacologically active compounds can be assessed quickly and easily by observing the total emission and CPL spectral changes of the chiral Eu(III) complex, $[Eu.L^1]^+$. Such information is important for dosage and treatment protocols, as the fraction of free and bound drug *in vivo* will depend on the concentration of AGP in serum, and this varies in a variety of disease states, notably in infection and inflammation. Given that related Eu(III) complexes have been used to monitor analytes like citrate, lactate and urate [16] in a wide range of bio-fluids, using relatively cheap instrumentation, such sensitive luminescence methods offer scope for development. Moreover, alpha-1-acid glycoprotein itself has been identified, following a study on17,345 patients, as one of only four key circulating 'biomarkers', that can be used to estimate the five-year risk of "all-cause" mortality. Indeed, α_1-AGP was stated to be 'the strongest multivariate predictor of the risk of death from all causes'. The other three biomarkers are citrate, albumin and the particle size of very low density lipoprotein. [17]

Experimental

The Eu complex was prepared as described earlier [12] : $\mathbf{[Eu.L^1(H_2O)]^+}$ *m/z* ($HRMS^+$) 855.1797 $[M]^+$ ($C_{38}H_{36}EuN_6O_8{}^{151}Eu$ requires 855.1816); (HPLC) t_R = 4.8 min; λ_{max} (H_2O) 336 nm.

HPLC analysis

Reverse-phase preparative HPLC used to purify the Eu complex was performed at 295 K using a Shimadzu system consisting of a Degassing Unit (DGU-20A5R), a

Prominence Preparative Liquid Chromatograph (LC-20AP), a Prominence UV/Vis Detector (SPD-20A) and a Communications Bus Module (CBM-20A). An XBridge C18 OBD 19 x 100 mm, i.d. 5 μM column was used with a flow rate of 2 mL/min (analytical) or 17 mL/min (prep). The solvent system was H_2O +0.1% formic acid / MeOH +0.1% formic acid (gradient elution, see Table 2). The UV detector was set at 336 nm and fraction collection was performed manually.

Table 2 HPLC conditions used for the purification of $[Eu.L^1(H_2O)]^+$.

Step	Time / min	Flow (Analytical/Prep) / mL min^{-1}	%H_2O (0.1% FA)	%MeOH (0.1% FA)
0	0.0	2.0 / 17.0	90.0	10.0
1	10.0	2.0 / 17.0	5.0	95.0
2	13.0	2.0 / 17.0	5.0	95.0
3	13.5	2.0 / 17.0	90.0	10.0
4	16.5	2.0 / 17.0	90.0	10.0

Optical methods All samples for optical analyses were contained in quartz cuvettes with a path length of 1 cm and a polished base. Measurements were recorded at 295 K. UV-Vis absorbance spectra were recorded on an ATI Unicam UV/Vis spectrometer (Model UV2) using Vision version 3.33 software. Samples were measured relative to a reference of pure solvent contained in a matched cell. Emission spectra were recorded on an ISA Joblin-Yvon Spex Fluorolog-3 luminescence spectrometer using DataMax v2.2.10 software. An integration time of 0.5 seconds and increment of 0.5 nm were used. Lifetime measurements were carried out on a Perkin Elmer LS55 spectrometer using custom written software. The Ln^{3+} ion was directly excited via the chromophore using a short pulse of light at λ_{exc} (336 nm for $[Eu.L^1(OH_2)]^+$), followed by monitoring the integrated intensity of the light emitted at a chosen wavelength (612.5 nm for Eu), during a fixed gate time, t_g, after a delay time, t_d. Measurements were made for a minimum of 20 delay times, covering more than 3 lifetimes. A gate time of 0.1 ms was used and the excitation and emission slits were set to 10 nm. The observed decay curves were plotted in Excel using eq. 1.

$$I = A_0 + A_1 e^{-kt} \quad (1)$$

The excited state lifetime, τ, is the inverse of the radiative decay rate constant, k.

Apparent binding constants were calculated by fitting equation 2 to emission or CPL data using Origin™ software and non-linear least squares regression analysis.

$$[X] = \frac{\frac{(F-F_0)}{(F_1-F_0)}/K + [Eu] * \frac{(F-F_0)}{(F_1-F_0)} - [Eu] * \left(\frac{(F-F_0)}{(F_1-F_0)}\right)^2}{1 - \frac{(F-F_0)}{(F_1-F_0)}}$$

$$Eu + X \leftrightarrow EuX \qquad K = \frac{[EuX]}{[X_f][Eu_f]}$$

(2)

where [X]: Total concentration of selected analyte in solution ; [Eu]: Total concentration of the complex; K: Binding constant ; F: Either intensity ratio of selected emission transitions or I_L - I_R values; F_0: Initial ratio; F_1: Final ratio; [EuX]: The concentration of the analyte-coordination complex; $[X_f]$: The concentration of free analyte; $[Eu_f]$: The concentration of free complex

The CPL spectra were recorded on a custom built spectrometer [15] consisting of a laser driven light source (Energetiq EQ-99 LDLS, spectral range 170 to 2100 nm) coupled to an Acton SP2150 monochromator (600 g/nm, 300 nm Blaze) that allows excitation wavelengths to be selected with a 6 nm FWHM band-pass. The collection of the emitted light was facilitated (90° angle set up, 1 cm path length quartz cuvette) by a Lock-In Amplifier (Hinds Instruments Signaloc 2100) and Photoelastic Modulator (Hinds Instruments PEM-90). The differentiated light was focused onto an Acton SP2150 monochromator (1200 g/nm, 500 nm Blaze) equipped with a high sensitivity cooled Photo Multiplier Tube (Hamamatsu 10723-01 red corrected).

The detection of the CPL signal was achieved using the field modulation lock-in technique. The electronic signal from the PMT was fed into the lock-in amplifier (Hinds Instruments Signaloc 2100). The reference signal for the lock-in detection was provided by the PEM control unit. The monochromators, PEM control unit and lock-in amplifier were interfaced with a desktop PC and controlled by Labview code.

A correction factor for the wavelength dependence of the detection system was

constructed using a calibrated lamp (Edmund Optics). The measured raw data was subsequently corrected using this correction factor. The validation of the CPL detection systems was achieved using light emitting diodes (LEDs) at various emission wavelengths. The LED was mounted in the sample holder and the light from the LED (650 nm) was fed through a broad-band polarising filter and quarter wave plate (Thor Labs) to generate circularly polarised light. Prior to all measurements, this technique was used to set the phase of the lock-in amplifier correctly. Spectra were recorded using a 5 spectral average sequence in the range of 570-720 nm (Eu), with 0.5 nm spectral intervals and using a 500 microsecond integration time.

Acknowledgments We thank the Royal Society (RP), FScan Ltd. and EPSRC (EP/I010319/1) for support.

References

1. K. Taguchi, K. Nishi, V. T. G. Chuang, T. Maruyama and M. Otagiri, *Acute Phase Proteins*, **2013**.

2. J. L. Behan, Y. E. Cruickshank, G. Matthews-Smith, M. Bruce and K. D. Smith, *Biomed Res. Int*., **2013**, 108902.

3. F. Zsila and Y. Iwao, *Biochim. Biophys. Acta*, **2007**, *1770*, 797–809.

4. K. Nishi, T. Ono, T. Nakamura, N. Fukunaga, M. Izumi, H. Watanabe, A. Suenaga, T. Maruyama, Y. Yamagata, S. Curry and M. Otagiri, *J. Biol. Chem.*, **2011**, *286*, 14427

5. a) G. L. Trainor, *Expert Opin. Drug Discovery*, **2007**, *2***,** 51; b) K. M. Wasan, D. R. Brocks, S. D. Lee, K. Sachs-Barrable and S. J. Thornton, *Nat. Rev. Drug Discovery*, **2008**, *7*, 84; c) F. Hervé, G. Caron, J.-C. Duché, P. Gaillard, N. Abd. Rahman, A. Tsantili-Kakoulidou, P.-A. Carrupt, P. d'Athis, J.-P. Tillement and B. Testa, *Mol. Pharmacol.,* **1998**, *54*, 129.

6. Methadone: F. P. Abramson, *Clin. Pharmacol. Ther*. **1982**, *32*, 652.

7. Imatinib: I. Fitos, J. Visy, F. Zsila, G. Mady, M. Simonyi, *Biochim. Biophys. Acta*, **2006**, *1760***,** 1704

8. Disopyramide: K. Hanada, T. Ohta, M. Hirai, M. Arai, H. Ogata*, J. Pharm. Sci*., **2000**, *89*, 751.

9. Lidocaine /Imipramine: a) H. Xuan and D. S. Hage, *Anal. Biochem*. **2005**, *346*, 300; b) S. Soman, M. J. Yoo, Y. J. Jang and D. S. Hage, *J. Chromatogr. B*, **2010**, *878*, 705.

10. Bupivacaine: a) S. Taheri, L. P. Cogswell, A. Gent and G. R. Strichartz, *J. Pharmacol. Exp. Ther.*, **2003**, *304*, 71–80; b) D. Denson, D. Coyle, G. Thompson and J. Myers, *Clin. Pharmacol. Ther*., **1984**, *35*, 409–15; c) J. X. Mazoit, L. S. Cao and K. Samii, *J. Pharmacol. Exp. Ther*., **1996**, *276*, 109–15.

11. Nortriptyline: M. Brinkschulte and U. Breyer-Pfaff, NaunynSchmiedebergs Arch. Pharmacol., **1980**, *314*, 61–66; M. J. Yoo and D. S. Hage, *J. Sep. Sci*., **2011**, *34*, 2255–2263.

12. R. Carr, L. Di Bari, S. Lo Piano, D. Parker, R. D. Peacock and J. M. Sanderson, *Dalton Trans*., **2012**, *41*, 13154–8.

13. a) For relevant reviews of CPL: F. Zinna and L. Di Bari, *Chirality,* **2015**, *27*, 1; J. P. Riehl and F. S. Richardson, *Chem. Rev*. **1986**, *86*, 1; R. Carr, N. H. Evans and D. Parker, *Chem. Soc. Rev*. **2012**, *41*, 7673; G. Muller, *Dalton Trans*. **2009**, 9692; T. Wu, X-Z. You, P. Bour, *Coord. Chem. Rev*. **2015**, *284*, 1; b) for selected examples using CPL to monitor reversible binding: E. R. Neil, M. A. Fox, R. Pal and D. Parker, *Dalton Trans*. **2016**, *45*, 8355; E. R. Neil, M. A. Fox, R. Pal, L-O. Palsson, B. A. O'Sullivan, D. Parker, *Dalton Trans*. **2015**, *44*, 14937; K. Okutani, K. Nozaki and M. Iwamura, *Inorg. Chem*., **2014**, *53*, 5527; D. G. Smith, B. K. McMahon, R. Pal, D. Parker, *Chem. Commun*., **2012**, *48*, 8520; D. G. Smith, R. Pal and D. Parker, *Chem. – Eur. J.*, **2012**, *18*,11604; C. P. Montgomery, E. J. New, D. Parker, R. D. Peacock, *Chem. Commun*. **2008**, 4261; S. C. J. Meskers and H. P. J. M. Dekkers, *J. Phys. Chem. A*, **2001**, *105*, 4589; S. C. J. Meskers, H. P. J. M. Dekkers, G. Rapene and J.-P. Sauvage, *Chem.–Eur. J*., **2000**, *6*, 2129; J. I. Bruce, R. S. Dickins, T. Gunnlaugsson, S. Lopinski, M. P. Lowe, D. Parker, R. D. Peacock, J. J. B. Perry, S. Aime and M. Botta, *J. Am. Chem. Soc*., **2000**, *122*, 9674; c) other recent examples of uses of CPL: B. Zercher, T. Hopkins, *Inorg. Chem*., **2016**, DOI: 10.1021/acs.inorgchem.6b01343. T. Wu, J. Průša, J. Kessler, M. Dračínský, J. Valenta, P. Bouř, *Anal. Chem*., **2016**, *88***,** 8878; M. Iwamura, Y. Kimura, R. Miyamoto, K. Nozaki, *Inorg Chem,* **2012**, *51*, 4094. J. Yuasa, T. Ohno, H. Tsumatori, R. Shiba, H. Kamikubo, M. Kataoka, Y. Hasegawa and T. Kawai, *Chem. Commun*., **2013**, *49*, 4604–4606, L. Dai, W. Lo, I. D. Coates, R. Pal and G. Law, *Inorg. Chem*., **2016**, *55*, 9065–9070.

14. F. Herve, G. Caron, J. C. Duche, P. Gaillard, N. Abdu Rahman, A. Tsantili-Kakoulidou, P. A. Carrupt, P. d'Athis, J. P. Tillement and B. Testa, *Mol Pharmacol*, **1998**, *54*, 129–138.

15. R. Carr, R. Puckrin, B. K. McMahon, R. Pal, D. Parker and L.-O. Pålsson, *Methods Appl. Fluoresc*., **2014**, *2,* 024007.

16. Citrate and lactate: R. Pal, D. Parker, L. C. Costello, *Org. Biomol. Chem*. **2009**, *7*, 1525; R. Pal, A. Beeby and D. Parker, *J. Pharmaceut. Biomed. Anal*, **2011**, *56*, 352; urate: R. A. Poole, F. Kielar, S. L. Richardson, R. Pal, D. Parker, *Chem. Commun*. **2006**, 4084.

17. K. Fischer, J. Kettunen, P Wurtz, T. Haller, A. S. Havulinna, A. J. Kangas, P. Soininen, T. Esko, M-L. Tammesco, R. Magi, S. Smit, A. Palotie, S. Ripatti, V. Salomaa, M. Ala-Korpela, M. Periola and A. Metspalu, *PLoS Med.* **2014**, *11*, e1001606.